

$O(4)$ Expansion of the Ladder Bethe-Salpeter Equation

Taco Nieuwenhuis and J. A. Tjon

*Institute for Theoretical Physics, University of Utrecht, Princetonplein 5,
P.O. Box 80.006, 3508 TA Utrecht, the Netherlands.*

January 25, 2018

The Bethe-Salpeter amplitude is expanded on a hyperspherical basis, thereby reducing the original 4-dimensional integral equation into an infinite set of coupled 1-dimensional ones. It is shown that this representation offers a highly accurate method to determine numerically the bound state solutions. For generic cases only a few hyperspherical waves are needed to achieve convergence, both for the ground state as well as for radially or orbitally excited states. The wave function is reconstructed for several cases and in particular it is shown that it becomes independent of the relative time in the nonrelativistic regime.

I. INTRODUCTION

Over the past 40 years the Bethe-Salpeter equation has been the traditional starting point for relativistic field theoretical studies of two-body bound states [1–3]. In view of the numerical complexity, most studies are restricted to the ladder approximation. Within this approximation the two-body amplitude obeys a 4-dimensional integral equation that can easily be transformed into a Fredholm-type eigenvalue problem by a Wick rotation [4]. Except for the Wick-Cutkosky model [4,5] where two scalar particles interact through the exchange of a massless particle, very limited analytically obtained information is known about the solutions of the ladder Bethe-Salpeter equation. Moreover, despite its fairly transparent structure, it has proven to be a nontrivial numerical problem to find accurate solutions of it for a more general type of interaction.

Many studies have been carried out to determine the Bethe-Salpeter eigenvalues and vertex functions numerically. Most efforts start with the reduction of the 4-dimensional integral equation into a 2-dimensional one by introducing a partial wave decomposition, thereby exploiting rotational symmetry [6,7]. The 2-dimensional integral equation is then solved by standard discretization methods. Although the resulting matrix equations can be solved numerically, one has often to deal with very large matrices, especially when the spin complication of the external particles has to be accounted for. In addition, this happens also when the exchanged mass becomes small. To account properly for the long range character of the interaction, a larger number of integration points is needed in that case. Variational calculations [8,9] have also been done and proven to be a powerful technique. They are, however, harder to apply to studies of excited states.

In this work we consider an alternative method for solving the ladder Bethe-Salpeter equation based on a hyperspherical expansion [10]. Instead of doing a standard partial wave decomposition, thereby expanding the amplitude on a basis of $O(3)$ spherical harmonics, we expand the amplitude on an $O(4)$ basis. As a result the ladder Bethe-Salpeter equation is transformed into an infinite set of coupled 1-dimensional integral equations. This representation clearly has the advantage that the integral equations are substantially easier and more accurately solvable, provided that the number of channels is limited. The idea behind this method is in fact quite old and some approximated, lowest order results have already been published a long time ago [11]. Here we will systematically improve upon the lowest order calculations and solve the full set of integral equations until the desired accuracy has been achieved. For typical

calculations only very few hyperspherical waves are needed in practice in order to find a reasonable accuracy. In particular when the exchanged mass or the binding energy is sizable as compared to the constituent masses, only 1 or 2 hyperspherical waves are required to reach convergence.

In Sect. II we discuss the ladder Bethe-Salpeter equation and introduce the hyperspherical expansion to derive the resulting coupled set of 1-dimensional integral equations. In Sect. III we present the numerical results. The rate of convergence of the eigenvalues and vertex functions is studied and shown to be fast which renders the method an efficient one. Finally, in Sect. IV we show that the method can also be used to reconstruct the solutions in the case of (2+1) dimensions and some concluding remarks are made. Two appendices contain the explicit expressions of the kernel of the Bethe-Salpeter equation on the hyperspherical basis, both for (3+1) as well as for (2+1) dimensions.

II. THE LADDER BETHE-SALPETER EQUATION

For definiteness, let us consider the bound state problem of two scalar particles with mass m in $(d-1)$ spatial and 1 time dimensions. In a relativistic field theory a two-particle bound state with mass M corresponds to a solution of the homogeneous Bethe-Salpeter equation (BSE) at total momentum P with $P^2 = M^2$. After a Wick rotation [4], the BSE for the corresponding vertex function $\Phi(q)$ has the general structure

$$\Phi(q) = \frac{1}{(2\pi)^d} \int d^d q' V(q, q') S(q') \Phi(q'), \quad (1)$$

where q is the relative momentum, $V(q, q')$ is the set of all 2-particle irreducible diagrams and $S(q)$ is the free 2-particle Green function. In the CM-frame ($P = (\mathbf{0}, \sqrt{s})$) we have for $S(q)$

$$\begin{aligned} S(q) &= \frac{1}{(q^2 + m^2 - \frac{1}{4}s)^2 + (q \cdot P)^2}, \\ &= \frac{1}{(q^2 + m^2 - \frac{1}{4}s)^2 + q^2 s \cos^2 \chi_{Pq}}, \end{aligned} \quad (2)$$

with χ_{Pq} being the angle between the (Euclidean) vectors P and q in d -dimensional momentum space. For a given $V(q, q')$, Eq. (1) only supports solutions for values of $\sqrt{s} < 2m$ that correspond to bound states.

In this paper we will confine ourselves to the particular example of two scalar particles with mass m , interacting through the exchange of another scalar particle with mass μ . In the ladder approximation we have

$$\begin{aligned} V(q, q') &= g^2 \frac{1}{(q - q')^2 + \mu^2}, \\ &= g^2 \frac{1}{q^2 + q'^2 + \mu^2 - 2|q||q'| \cos \gamma_{qq'}}, \end{aligned} \quad (3)$$

with $\gamma_{qq'}$ the angle between the relative momenta q and q' . Eq. (1) sums up the set of ladder diagrams depicted in Fig. 1. In this work we focus our attention to the (3+1)-dimensional case. Appendix B contains the essential expressions for the (2+1)-dimensional case and the generalization to other space-time dimensions can be made analogously.

Usually Eqs. (1-3) are solved by noting that for $d = 4$ they exhibit $O(3)$ -symmetry and as a result it is profitable to expand the amplitudes on a basis of $O(3)$ spherical harmonics $Y_{lm}(\theta, \phi)$. This reduces the ladder BSE to a 2-dimensional integral equation in the 3-momentum $|\mathbf{q}|$ and the relative energy variable q_4 . Since for $s = 0$ the BSE has an additional $O(4)$ -symmetry, which as a consequence reduces it to a single 1-dimensional integral equation in

that particular case, it is tempting to explore the convergence rate of an expansion in terms of hypersphericals in 4 dimensions. Such a method should in particular work very well for the case of strong binding. Starting from Eq. (1) we may expand the vertex function $\Phi(q)$ in appropriate 4-dimensional spherical harmonics. From Eq. (2) it is clear that for $s \neq 0$ the BSE-kernel is not $O(4)$ invariant. Hence the expansion in hyperspherical harmonics will not lead to a complete separation of the generalized angular variables.

In (3+1) dimensions the suitable set of spherical harmonics is given by:

$$Z_{klm}(\chi, \theta, \phi) = X_{kl}(\chi) Y_{lm}(\theta, \phi), \quad (4)$$

with

$$X_{kl}(\chi) \equiv \sqrt{\frac{2^{l+1}}{\pi} \frac{(k+1)(k-l)!l!^2}{(k+l+1)!}} \sin^l \chi C_{k-l}^{l+1}(\cos \chi), \quad (5)$$

$$Y_{lm}(\theta, \phi) \equiv (-1)^m \sqrt{\frac{2l+1}{4\pi} \frac{(l-m)!}{(l+m)!}} P_l^m(\cos \theta) e^{im\phi}. \quad (6)$$

Here $C_{k-l}^{l+1}(x)$ are the Gegenbauer polynomials of degree $k-l$ and order $l+1$ and $P_l^m(x)$ are the associated Legendre functions of the first kind of degree l and order m [12]. For a fixed value of k , the index l assumes integer values from 0 to k , while m goes from $-l$ to l . Standard properties of these functions allow one to prove completeness and orthogonality for the set $Z_{klm}(\chi, \theta, \phi)$ with respect to the scalar product at hand

$$\int_0^{2\pi} d\phi \int_0^\pi d\theta \sin \theta \int_0^\pi d\chi \sin^2 \chi Z_{klm}(\chi, \theta, \phi) Z_{k'l'm'}^*(\chi, \theta, \phi) = \delta_{kk'} \delta_{ll'} \delta_{mm'}. \quad (7)$$

By expanding $\Phi(q)$ and $V(q, q')$ in Eq. (1) as

$$\Phi(q) = \sum_{klm} \Phi_{klm}(|q|) Z_{klm}(\chi, \theta, \phi) \quad (8)$$

$$V(q, q') = \sum_k V_k(|q|, |q'|) C_k^1(\cos \gamma_{qq'}) \quad (9)$$

and using the addition theorem for the 4-dimensional hyperspherical harmonics

$$C_k^1(\cos \gamma) = \frac{2\pi^2}{k+1} \sum_{lm} Z_{klm}(\chi, \theta, \phi) Z_{klm}^*(\chi', \theta', \phi'), \quad (10)$$

where γ is the angle between the two unit vectors (χ, θ, ϕ) and (χ', θ', ϕ') , we obtain after some straightforward algebra an infinite set of coupled 1-dimensional integral equations:

$$\Phi_{klm}(q) = \frac{1}{8\pi^2(k+1)} \sum_{k'} \int_0^\infty dq' q'^3 V_k(q, q') S_{kk'}^l(q') \Phi_{k'lm}(q'). \quad (11)$$

Here the matrix $S_{kk'}^l(q)$ is given by

$$S_{kk'}^l(q) = \int_0^\pi d\chi \sin^2 \chi X_{kl}(\chi) X_{k'l}(\chi) S(|q|, \cos \chi). \quad (12)$$

For our particular case the matrix-elements $V_k(q, q')$ and $S_{kk'}^l(q)$ can explicitly be computed and are given in Appendix A.

Eq. (11) exhibits several symmetries that allow for a physical interpretation and which lead to simplifications in the numerical treatment. Since $V_k(q, q')$ and $S_{kk'}^l(q)$ are independent of the magnetic quantum number m , the solutions of

(11) do not depend on it. Hence there is a $(2l+1)$ -fold degeneracy present which is a manifestation of the cylindrical symmetry. Furthermore, Eq. (11) is diagonal in the orbital quantum number l which implies the conservation of spatial angular momentum, in contrast to the nonconservation of the generalized angular momentum connected to the quantum number k . Considering the behavior under parity transformations $x \rightarrow -x$ of the Gegenbauer polynomials: $C_{k-l}^{l+1}(-x) = (-1)^{k-l} C_{k-l}^{l+1}(x)$ leads to the conclusion that $S_{kk'}^l(q)$ is only nonzero if $k+k'$ is even. As a result only states of equal parity are coupled to each other in (11) and consequently parity is conserved. Finally, one can show that $S_{kk'}^l(q)$ vanishes unless $k \geq l$ and $k' \geq l$. Hence, for a fixed value of l , the quantum numbers of the generalized angular momentum assume values $k = l + 2j$ and $k' = l + 2j'$, with $j \in 0, 1, 2, \dots$.

III. NUMERICAL RESULTS

Having transformed the original 4-dimensional integral equation (1) into an infinite set of coupled 1-dimensional ones, our aim is now to find those values of $s < 4m^2$ for which Eq. (11) allows solutions. As noted these would correspond to bound states with mass $M = \sqrt{s}$. In particular it is interesting to investigate how many hyperspherical waves are required in order to achieve a certain accuracy and to see how this number depends on the properties of the particular state one is considering.

A. Numerical Implementation

In order to evaluate the integral in Eq. (11), we project the infinite interval $q = [0, \infty)$ on to the finite unit interval $z = [0, 1]$ through the transformation: $q \rightarrow z/(1-z)$. The integral can then simply be computed by Gauss-Legendre quadratures [13].

$$\int_0^1 dx f(x) = \lim_{N \rightarrow \infty} \sum_{i=1}^N w_i f(x_i), \quad (13)$$

with weights w_i and abscissas x_i . Next we truncate the infinite sum over k' in Eq. (11) at a finite value of $k' = k_{\max}$. As a result we have replaced the kernel of the integral equation by an approximated finite matrix \mathbf{K} of dimension $(N \cdot k_{\max}) \times (N \cdot k_{\max})$ of which we seek the eigenvalues. After having computed $\det(\mathbf{1} - \mathbf{K})$ numerically, we apply Newton's method [13] in order to find the roots of $\det(\mathbf{1} - \mathbf{K})$ as a function of \sqrt{s} for a fixed value of g or vice versa. Typical values of $N = 60$ have been used in the actual calculations, except for the case of smallest μ , where $N = 200$ was needed to get the same relative accuracy as the other ones. Finally we checked for a large number of states that we obtained identical results as zur Linden [14].

B. Convergence of the Eigenvalues

Since the BSE is only $O(4)$ -invariant for $\sqrt{s} = 0$, the rate of convergence of the hyperspherical method is expected to show a significant dependence on the value of the bound state mass $\sqrt{s} \equiv M$. We study the convergence rate by keeping M fixed at different values and determining the value of the dimensionless coupling constant $\lambda = g^2/4\pi m^2$ that yields a bound state of these masses.

In Table I we present a comparison of calculations for different values of M and μ . For the calculations we consider the ground state where the radial quantum number $n = 1$ and the system is in an s -state ($l = 0$). We indeed find for a given μ that a larger value of k_{\max} is required for increasing M in order to obtain a certain accuracy. Except for the smallest value of $\mu/m = 0.001$ and the weak binding case of $M/m = 1.999$, it is remarkable to see how fast the method converges. The latter exceptional case corresponds to the nonrelativistic situation where the binding is small as compared to the rest masses of the constituents. A reasonable relative accuracy of 10^{-4} can rather easily be obtained by considering only a few hyperspherical waves. The convergence is extremely good for moderate values of $\mu/m \simeq 1$ where only two hyperspherical waves suffice for the desired accuracy. Comparing the predictions for the case of $\mu/m = 0.001$ with those of the Wick-Cutkosky model we find that they agree within 4 digits, except for the weak binding situation $M/m = 1.999$. The poorer correspondence for the latter case is understandable since the exchange mass, which vanishes in the Wick-Cutkosky case, is of the order of the binding energy of the system here. Hence its influence on the long range structure of the bound state is expected to be significant, while it is negligible for the other situations.

Next we wish to study how the above pattern depends on the orbital quantum number l . For this investigation we keep μ fixed at $\mu/m = 0.1$ and we vary l at different values of the bound state mass M . The results of this calculation is presented in Table II. From this table we see, for each value of M , that the rate of convergence is virtually independent of the orbital quantum number l .

Finally, solutions of radially excited states have been studied. Some results are shown in Table III. Also in this case we find that the hyperspherical method works very well. The convergence rate is found to be only very weakly dependent on the radial quantum number n .

From the above investigations, we may conclude that for the computation of the spectrum, the rate of convergence of the hyperspherical method is, as expected, dependent on the bound state mass M and on the value of the exchanged mass μ . The convergence rate is in general very fast except for small values of the exchanged mass μ . This is not surprising since again we expect that the long range character of the force for $\mu \rightarrow 0$ should be reflected in the rate of convergence. In this connection, it should be noted that keeping a finite number of the hyperspherical waves, the resulting kernel of the BSE is compact even in the limit $\mu \rightarrow 0$. For performing the integrals in an accurate way, more integration points are needed when μ becomes small. This may be attributed to the appearance of a cusp in $V_k(q, q')$ at $q = q'$ when μ is identically 0.

C. Hyperspherical Components of the Wave Functions

Clearly, the BSE (1) with kernel \mathbf{K} has formally the structure of a generalized eigenvalue problem

$$\lambda \Phi = \mathbf{K} \Phi. \quad (14)$$

After discretization of the integral in the BSE we may find for a given energy \sqrt{s} the eigenvalues and eigenvectors of the matrix \mathbf{K} using standard procedures. The physical solutions can simply be obtained by varying s such that we get an eigenvalue $\lambda = 1$. Once the eigenvectors have been determined of Eq. (14) we immediately obtain the wave function $\Psi(q)$ through the relation

$$\Psi(q) = S(q)\Phi(q) \quad (15)$$

In the actual reconstruction of the ground state vertex function we have used the so-called power method [15], which is considerably faster than the procedures for obtaining general eigenvectors. It simply consists of the iteration procedure

$$\Phi^{(n+1)} = \mathbf{K}\Phi^{(n)}. \quad (16)$$

One can readily show, that the limiting function $\Phi^{(n \rightarrow \infty)}$ becomes proportional to the eigenvector with largest eigenvalue λ . This eigenvalue is simply given by $\lambda = \lim_{n \rightarrow \infty} \Phi^{(n+1)}/\Phi^{(n)}$. To accelerate the iterative procedure we have chosen a starting vector $\Phi^{(0)}$ which incorporates the asymptotic behavior of the different hyperspherical waves

$$\Phi_{k0}(q) \xrightarrow{q \rightarrow 0} q^k, \quad (17)$$

$$\xrightarrow{q \rightarrow \infty} q^{-k-2}, \quad (18)$$

More specifically, we choose $\Phi_{k0}^{(0)}(q)$ according to:

$$\Phi_{k0}^{(0)}(q) = \frac{q^k}{(1+q^2)^{k+1}}. \quad (19)$$

The method was used as an additional check on all numerically obtained eigenvalues.

Obviously the eigenvectors can be obtained in this way up to a normalization. We have normalized the wave functions according to the well known BSE normalization condition given by [2]

$$\int \frac{d^4q}{(2\pi)^4} \frac{d^4q'}{(2\pi)^4} \Psi(q) \frac{\partial}{\partial P_\mu} [(2\pi)^4 \delta^4(q - q') S^{-1}(q) + V(q, q')] \Psi^*(q') = 2P_\mu \quad (20)$$

Inserting the expansion (8) in (20) we find in the CM-frame for each partial wave l :

$$\frac{1}{2(2\pi)^4} \sum_{kk'} \int_0^\infty dq q^3 \Psi_{kl}(q) [2q^2 A_{kk'}^l - \delta_{kk'} (q^2 + m^2 - \frac{1}{4}s)] \Psi_{k'l}(q) = 1 \quad (21)$$

where we have defined:

$$\Psi_{kl}(q) = \sum_{k'} S_{kk'}^l(q) \Phi_{k'l}(q) \quad (22)$$

$$A_{kk'}^l = \int_0^\pi d\chi \sin^2 \chi X_{kl}(\chi) X_{k'l}(\chi) \cos^2 \chi \quad (23)$$

In Appendix A the explicit expression for $A_{kk'}^l$ is given.

In Fig. 2 we show as typical examples the rate of convergence of the hyperspherical method for the vertex function $\Phi(|\mathbf{q}|, q_4)$ of the ground state for two values of the relative energy q_4 in the case of a bound state mass $M = 1.9m$. For the whole $|\mathbf{q}| - q_4$ region we need only 4 hyperspherical waves for this case to get a reasonably converged result for the vertex function. As we can see from Fig. 3, the $|\mathbf{q}|$ - and q_4 -dependence of the calculated Φ are smooth and the range of fall-off in these two variables are similar.

The rapid convergence of the hyperspherical method is related to the magnitude of the hyperspherical components in the wave function. In Fig. 4 we display for $l = 0$ and $\mu/m = 0.1$ the components of the ground state wave function for the cases $M/m = 1$ and 1.9 . The corresponding coupling constants are given by $\lambda = 20.678$ respectively $\lambda = 5.227$. For the latter case we see that the contributions of higher ($k \geq 2$) hyperspherical waves are indeed more significant than for the former situation, in agreement with the slower rate of convergence of the eigenvalue. Moreover, from the

figure we see that the range of the fall-off in q is very different for the two cases. This is predominantly caused by the s -dependence of the free 2-particle Green function and related to the size of the composite system. The hyperspherical components of the corresponding vertex functions exhibit a more comparable range and the non-leading ones are relatively more suppressed in magnitude.

In the weak binding regime we expect both particles to be nearly on their mass-shell, which results for the wave function Ψ in a strongly peaked structure in the q_4 -variable as compared to the typical fall-off in the $|\mathbf{q}|$ -variable. As a consequence we expect that the wave function in the configuration space will exhibit an independence on the relative time t in the nonrelativistic limit. We have studied this transition region. The wave functions in configuration space can be obtained from the above ones via Fourier transformation. With the help of the representation of the complex exponential

$$e^{iq \cdot r} = 4\pi^2 \sum_{klm} \frac{J_{k+1}(qr)}{qr} Z_{klm}(\chi_q, \theta_q, \phi_q) Z^*(\chi_r, \theta_r, \phi_r), \quad (24)$$

we find that for a fixed l , the configuration space wave functions are given by

$$\Psi_l(|\mathbf{r}|, t) = \frac{1}{4\pi^2 \sqrt{\mathbf{r}^2 + t^2}} \sum_k i^k X_{kl} \left(\arccos \frac{t}{\sqrt{\mathbf{r}^2 + t^2}} \right) \int_0^\infty dq \ q^2 J_{k+1} \left(q \sqrt{\mathbf{r}^2 + t^2} \right) \Psi_{kl}(q) \quad (25)$$

The integral Eq. (25) was performed by Gauss-Legendre integration. In order to compute the wave functions $\Psi_l(|\mathbf{r}|, 0)$ at relative time zero, one needs the value of $X_{kl}(\frac{1}{2}\pi)$

$$C_{k-l}^{l+1}(0) = (-1)^{\frac{1}{2}(k-l)} \binom{\frac{1}{2}(k+l)}{\frac{1}{2}(k-l)} \implies X_{kl}(\frac{1}{2}\pi) = (-1)^{\frac{1}{2}(k-l)} \sqrt{\frac{2^{l+1}}{\pi} \frac{(k+1)(k-l)!(\frac{1}{2}(k+l))!}{(k+l+1)!(\frac{1}{2}(k-l))!}} \quad (26)$$

whereas the determination of the wave function $\Psi_l(0, t)$ at zero relative distance requires $X_{kl}(0)$

$$C_{k-l}^{l+1}(1) = \delta_{l0}(k+1) \implies X_{kl}(0) = \delta_{l0} \sqrt{\frac{2}{\pi}}(k+1), \quad (27)$$

We display in Fig. 5 the computed configuration space components

$$\hat{\Psi}_{kl}(r) = \frac{1}{4\pi^2 r} \int_0^\infty dq \ q^2 J_{k+1}(qr) \Psi_{kl}(q) \quad (28)$$

of the ground state, again for $M/m = 1.0$ and 1.9 with $\mu/m = 0.1$. Comparing this with Fig. 4 we see that the pronounced structure of the higher components is relatively more suppressed and its strength is spread out to larger values of \mathbf{r} . The asymmetric behaviour of the configuration space wave function Ψ_l from Eq. 25 as a function of $|\mathbf{r}|$ and t can clearly be seen in Fig. 6 for the case of $M/m=1.9$, $l=0$. Its fall-off in t is twice as slow as compared to that in $|\mathbf{r}|$.

Finally, it is of some interest to study the role of the relative time in the transition region to weak binding. In Fig. 7 we show three graphs with $M/m = 1, 1.9$ and 1.999 where we compare the dependence on the Euclidean relative time t to that of the relative distance $|\mathbf{r}|$. We expect that in going to the region where the binding energy becomes negligible as compared to the total mass of the system, to recover the Schrödinger wave functions and to lose the dependence on the relative time which is inherently absent in a nonrelativistic description. For $M/m \rightarrow 2$ we indeed observe that the dependence of $\Psi_0(|\mathbf{r}|, t)$ on t becomes substantially weaker as compared to that on \mathbf{r} , i.e., the wave functions clearly show the expected independence on the relative time t .

IV. CONCLUDING REMARKS

We have investigated the hyperspherical expansion for solving the ladder Bethe-Salpeter equation in (3+1) dimensions. It was found that it constitutes a powerful and efficient method for obtaining an accurate determination of the eigenvalues as well as the eigenfunctions. This is true both for the ground state as well as for excited states. We stress that all calculations presented here took at most one minute of CPU-time on a HP735-workstation. Except for the limiting cases of vanishing exchange mass or small binding energy, only a few hyperspherical waves suffice for computing the solutions to the ladder Bethe-Salpeter equation within an accuracy that is sufficient for most practical purposes. Furthermore, it was found that the eigenfunctions could be reconstructed in a straightforward fashion.

The method can equally well be generalized to the case of d -dimension. In particular, we may consider the case of 2 spatial and 1 time dimensions. The explicit form of the kernel of the BSE for this case is given in Appendix B. In Table IV we show the converged results for the dimensionless coupling constant $\lambda = g^2/4\pi m$ for fixed values of the bound state mass and $\mu \rightarrow 0$. Similar rates of convergence properties are found as for the (3+1) dimensional case, i.e., for weak binding and smaller exchange mass μ more terms in the hyperspherical expansion are needed. From Table IV we see that the limit of $\mu \rightarrow 0$ is smooth and no logarithmic confinement is found, as would have been expected from a nonrelativistic analysis. Such a logarithmic behavior can readily be seen using the frequently adopted procedure to obtain a static nonrelativistic potential $V_{\text{NR}}(|\mathbf{r}|)$ from a relativistic interaction:

$$V_{\text{NR}}(|\mathbf{r}|) \equiv \int_{-\infty}^{\infty} dt V(|\mathbf{r}|, t). \quad (29)$$

For the Yukawa interaction in (2+1) dimensions we find consequently:

$$V_{\text{NR, Yukawa}}(|\mathbf{r}|) = -\frac{g^2}{2\pi} K_0(\mu|\mathbf{r}|). \quad (30)$$

The asymptotic behavior of the Bessel function for small arguments $K_0(z) \sim -\log(\frac{1}{2}z)$, suggests clearly that the nonrelativistic Coulomb interaction in (2+1) dimensions is logarithmically confining. According to table IV we find however the limiting behavior of $\mu \rightarrow 0$ to be smooth for the relativistic ladder BSE. Hence no confinement is seen in that limit. This paradoxical situation was investigated in [16] where it is found that a nonuniformity exists between the nonrelativistic limit $m \rightarrow \infty$ and the Coulomb limit $\mu \rightarrow 0$.

Given the very encouraging results we found in this study of scalar particles, we expect the hyperspherical expansion to be a powerful and accurate method to solve more realistic physical models such the ones that include spin degrees of freedom. In particular, we do expect that it can equally well be applied with good convergence properties for cases like the spinor-spinor interaction. Moreover, it should be interesting to investigate the applicability of the method to the scattering case.

APPENDIX A: HYPERSPHERICAL PROJECTION OF THE BSE₃₊₁

In this appendix we give the explicit formulae for the kernel of the (3+1) dimensional BSE that occur in the hyperspherical expansion. Most expressions are obtained with the help of standard properties of special functions, as can be found, e.g., in Ref. [12,17,18]

The projection of the interaction on the hyperspherical basis can be performed analytically

$$\begin{aligned}
V_k(q, q') &= g^2 \frac{2}{\pi} \int_0^\pi d\chi \sin^2 \chi C_k^1(\cos \chi) V(q, q', \cos \chi) \\
&= g^2 \frac{4}{(\Lambda_+ + \Lambda_-)^2} \left(\frac{\Lambda_+ - \Lambda_-}{\Lambda_+ + \Lambda_-} \right)^k
\end{aligned} \tag{A1}$$

where $\Lambda_\pm \equiv \sqrt{(q \pm q')^2 + \mu^2}$.

Substituting Eq. (5) in Eq. (12) and introducing $x = \cos \gamma_{Pq}$, we may rewrite $S_{kk'}^l(q)$ as

$$S_{kk'}^l(q) = \frac{2^{l+1} l!^2}{\pi} \sqrt{\frac{(k+1)(k-l)!}{(k+l+1)!}} \sqrt{\frac{(k'+1)(k'-l)!}{(k'+l+1)!}} \int_{-1}^1 dx (1-x^2)^{l+1/2} C_{k-l}^{l+1}(x) C_{k'-l}^{l+1}(x) S(q, x). \tag{A2}$$

After some tedious algebra this reduces to

$$S_{kk'}^l(q) = \frac{2\sqrt{2}i l!}{z\sqrt{\pi}} \sqrt{\frac{(k+1)(k-l)!}{(k+l+1)!}} \sqrt{\frac{(k'+1)(k'-l)!}{(k'+l+1)!}} e^{-(\frac{1}{2}l-\frac{1}{4})\pi i} (1+z^2)^{\frac{1}{2}l+\frac{1}{4}} C_{k+}^{l+1}(iz) Q_{k-+l+\frac{1}{2}}^{l+\frac{1}{2}}(iz) \tag{A3}$$

with

$$z \equiv \frac{q^2 + m^2 - \frac{1}{4}s}{q\sqrt{s}} \tag{A4}$$

and $k_+ \equiv \max(k, k')$ and $k_- \equiv \min(k, k')$. Despite the appearance of the imaginary unit ‘i’ in Eq. (A3), $S_{kk'}^l(q)$ is always real. For $l=0$ a more transparent form can be found from (A3).

$$S_{kk'}^0(q) = (-1)^{(k_+ - k_-)/2} \frac{1}{sq^2 z \sqrt{1+z^2}} \left[\left(\sqrt{1+z^2} - z \right)^{k_+ + k_- + 2} + (-1)^{k_-} \left(\sqrt{1+z^2} + z \right)^{k_+ - k_-} \right] \tag{A5}$$

The matrix-element $A_{kk'}^l$, defined in Eq. (23) as the expectation value of the operator $\cos^2 \chi$ between two spherical harmonics, can be computed with the help of the recurrence relation for Gegenbauer polynomials

$$2(n+m+1)x C_{n+1}^m(x) = (n+2m) C_n^m(x) + (n+2) C_{n+2}^m(x), \tag{A6}$$

which yields the following expression for $A_{kk'}^l$

$$\begin{aligned}
A_{kk'}^l &= \frac{1}{4} \left[\delta_{k,k'} \left(\frac{(k-l)(k+l+1)}{k(k+1)} + \frac{(k-l+1)(k+l+2)}{(k+1)(k+2)} \right) \right. \\
&\quad \left. + \delta_{k,k'+2} \frac{(k-l)(k+l+1)(k'-l+1)(k'+l+2)}{k(k+1)(k'+1)(k'+2)} + k \leftrightarrow k' \right]
\end{aligned} \tag{A7}$$

APPENDIX B: HYPERSPHERICAL PROJECTION OF THE BSE₂₊₁

In (2+1) dimensions the spherical harmonics are the $Y_{lm}(\theta, \phi)$ functions. The projection of the ladder BSE in this case closely follows that of the (3+1) dimensional case. After expanding the vertex function and the interaction on the hyperspherical basis

$$\Phi(q) = \sum_{lm} \Phi_{lm}(q) Y_{lm}(\theta, \phi), \tag{B1}$$

$$V(q, q') = \sum_l V_l(|q|, |q'|) P_l(\cos \gamma_{qq'}), \tag{B2}$$

and applying the appropriate addition theorem

$$P_l(\cos \gamma) = \frac{4\pi}{2l+1} \sum_m Y_{lm}(\theta, \phi) Y_{lm}^*(\theta', \phi') \quad (B3)$$

we find

$$\Phi_{lm}(q) = \frac{1}{2\pi^2(2l+1)} \sum_{l'} \int_0^\infty dq' q'^2 V_l(q, q') S_{ll'}^m(q') \Phi_{l'm}(q'). \quad (B4)$$

In Eq. (B4) the matrix $S_{ll'}^m(q)$ is defined analogously to Eq. (12)

$$S_{ll'}^m(q) = \int_0^\pi d\theta \sin \theta P_l^m(\cos \theta) P_{l'}^m(\cos \theta) S(|q|, \cos \theta). \quad (B5)$$

Similar considerations concerning conservation of angular momentum (with quantum number m) and parity as have been made earlier for the (3+1) dimensional case, apply here as well.

For the one meson exchange diagram we have

$$\begin{aligned} V_l(q, q') &= \frac{2l+1}{2} \int_0^\pi d\theta \sin \theta P_l(\cos \theta) V(q, q', \cos \theta) \\ &= g^2 \frac{2l+1}{2qq'} Q_l \left(\frac{q^2 + q'^2 + \mu^2}{2qq'} \right) \end{aligned} \quad (B6)$$

Moreover, the free 2-particle Green function with $m = 0$, $S_{ll'}^0(q)$, can be evaluated analytically:

$$S_{ll'}^0(q) = \frac{\sqrt{2l+1}\sqrt{2l'+1}}{4\pi i} \frac{1}{sq^2 z} P_{l-}(iz) Q_{l+}(iz), \quad (B7)$$

where z is defined in Eq. (A4), while l_\pm are defined according to $l_+ = \max(l, l')$ and $l_- = \min(l, l')$. Unfortunately, we were unable to find an analytical expression for $S_{ll'}^m(q)$ for arbitrary m . For $m \neq 0$, the integral in Eq. (B5) was performed numerically.

- [1] H. A. Bethe and E. E. Salpeter: ‘*Quantum Mechanics of One and Two Electron Atoms*’. Springer-Verlag 1957.
- [2] N. Nakanishi: Prog. Theor. Phys. Suppl. **43**, (1969) 1; ibid. **95**, (1988) 1.
- [3] C. Itzykson and J. B. Zuber: ‘*Quantum Field Theory*’. McGraw-Hill 1985.
- [4] G. C. Wick: Phys. Rev. **96**, (1954) 1124.
- [5] R. E. Cutkosky: Phys. Rev. **96**, (1954) 1135.
- [6] M. J. Levine, J. Wright and J. A. Tjon: Phys. Rev. **154**, (1967) 1433.
- [7] M. J. Zuilhof and J. A. Tjon: Phys. Rev. **C22**, (1980).
- [8] C. Schwartz: Phys. Rev. **137B**, (1965) 717.
- [9] S. H. Vosko: J. Math. Phys. **1**, (1960) 505. 2369.
- [10] M. Fabre de la Ripelle, Ann. Phys. (N.Y.) **197**, 2812 (1983).
- [11] M. Gourdin: Nuovo Cimento **7**, (1958) 338; M. Gourdin and J. Tran Thanh Van: ibid. **14**, (1959) 3955; ibid. **18**, (1960) 3667.
- [12] M. Abramowitz and I. A. Stegun: ‘*Handbook of Mathematical Functions*’. Dover Publications 1972.
- [13] W. H. Press, S. A. Teukolsky, W. T. Vetterling and B. P. Flannery: ‘*Numerical Recipes in FORTRAN*’. Cambridge University Press 1992.
- [14] E. zur Linden: Nuovo Cimento **61B**, (1969) 389; ibid. **63A**, (1969) 181; ibid. 193.
- [15] R.A. Malfliet and J.A. Tjon: Nucl. Phys. **A127** (1969) 391.
- [16] Taco Nieuwenhuis and J. A. Tjon: Phys. Lett. **B355** (1995) 283; Taco Nieuwenhuis, Ph. D. thesis, University of Utrecht, 1995.
- [17] A. P. Prudnikov, Yu. A. Brychkov and O. I. Marichev: ‘*Integrals and Series*’ vol. 2 & 3. Gordon and Breach 1990.
- [18] I. S. Gradshteyn and I. M. Ryzhik: ‘*Table of Integrals, Series and Products*’. Academic Press 1980.

TABLE I. Convergence of hyperspherical eigenvalues for $\lambda = g^2/4\pi m^2$ as a function of μ/m for $n = 1$ and $l = 0$. The numerical errors are at most one unit in the last decimal. When no further values are given for increasing k_{\max} , the final value was found not to change anymore within the desired accuracy when k_{\max} was increased. The case of $\mu/m = 0$ is the Wick-Cutkosky prediction.

μ/m	k_{\max}	$M/m = 0$	$M/m = 1$	$M/m = 1.9$	$M/m = 1.999$
0	—	25.13	20.01	4.483	0.2854
0.001	0	25.13	20.02	4.675	0.3484
	2		20.01	4.503	0.3099
	4			4.486	0.2992
	6			4.483	0.2947
	8				0.2924
	10				0.2912
	12				0.2904
	14				0.2899
	16				0.2896
	18				0.2894
	20				0.2893
	22				0.2892
	24				0.2891
	26				0.2890
0.100	0	25.80	20.69	5.374	1.0733
	2		20.68	5.237	1.0463
	4			5.228	1.0442
	6			5.227	1.0439
	8				1.0439
	10				1.0438
1.000	0	42.96	36.94	17.28	10.272
	2			17.23	10.251

TABLE II. Convergence of hyperspherical eigenvalues for $\lambda = g^2/4\pi m^2$ as a function of the orbital quantum number l for $n = 1$ and $\mu/m = 0.1$. The numerical errors are at most one unit in the last decimal. When no further values are given for increasing k_{\max} , the final value was found not to change anymore within the desired accuracy when k_{\max} was increased.

l	k_{\max}	$M/m = 0$	$M/m = 1$	$M/m = 1.9$	$M/m = 1.999$
0	0	25.802	20.678	5.3743	1.0733
	2			5.2369	1.0463
	4			5.2279	1.0442
	6			5.2271	1.0439
	8			5.2270	1.0439
	10				1.0438
1	1	160.44	127.48	33.284	10.086
	3			32.094	9.5620
	5			32.000	9.5043
	7			31.991	9.4957
	9			31.990	9.4942
	11				9.4940
	13				9.4939
2	2	668.88	531.01	143.58	55.385
	4			137.99	51.611
	6			137.51	51.123
	8			137.46	51.042
	10			137.45	51.027
	12				51.024
	14				51.023
3	3	2332.0	1856.2	525.81	237.45
	5			505.29	219.63
	7			503.44	217.12
	9			503.25	216.67
	11			503.23	216.59
	13				216.57

TABLE III. Convergence of hyperspherical eigenvalues for $\lambda = g^2/4\pi m^2$ as a function of the radial excitation quantum number n for $l = 0$ and $\mu/m = 0.1$. The numerical errors are at most one unit in the last decimal. When no further values are given for increasing k_{\max} , the final value was found not to change anymore within the desired accuracy when k_{\max} was increased.

n	k_{\max}	$M/m = 0$	$M/m = 1$	$M/m = 1.9$	$M/m = 1.999$
1	0	25.802	20.691	5.3743	1.0733
	2		20.678	5.2369	1.0463
	4			5.2279	1.0442
	6			5.2271	1.0439
	8			5.2270	1.0439
	10				1.0438
2	0	80.900	64.436	16.984	4.5741
	2		64.388	16.424	4.2927
	4		64.387	16.387	4.2578
	6			16.384	4.2521
	8			16.383	4.2510
	10				4.2508
3	0	169.55	135.84	38.053	12.111
	2		134.77	35.557	10.874
	4		134.74	35.257	10.715
	6			35.221	10.690
	8			35.217	10.686
	10			35.216	10.685

TABLE IV. Behavior of the eigenvalues of the BSE in (2+1) dimensions as $\mu \rightarrow 0$. The calculations are for the ground state.

μ/m	$M/m = 1.0$	$M/m = 1.9$
0.1000	2.869	0.3397
0.0300	2.477	0.2232
0.0100	2.366	0.1902
0.0030	2.328	0.1785
0.0010	2.314	0.1750
0.0003	2.308	0.1738
0.0001	2.305	0.1732

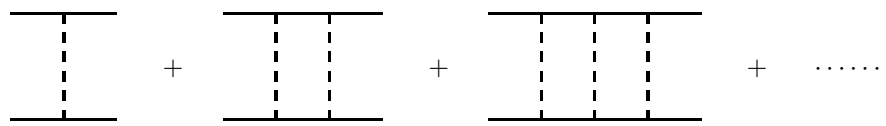


FIG. 1. General structure of the ladder diagrams.

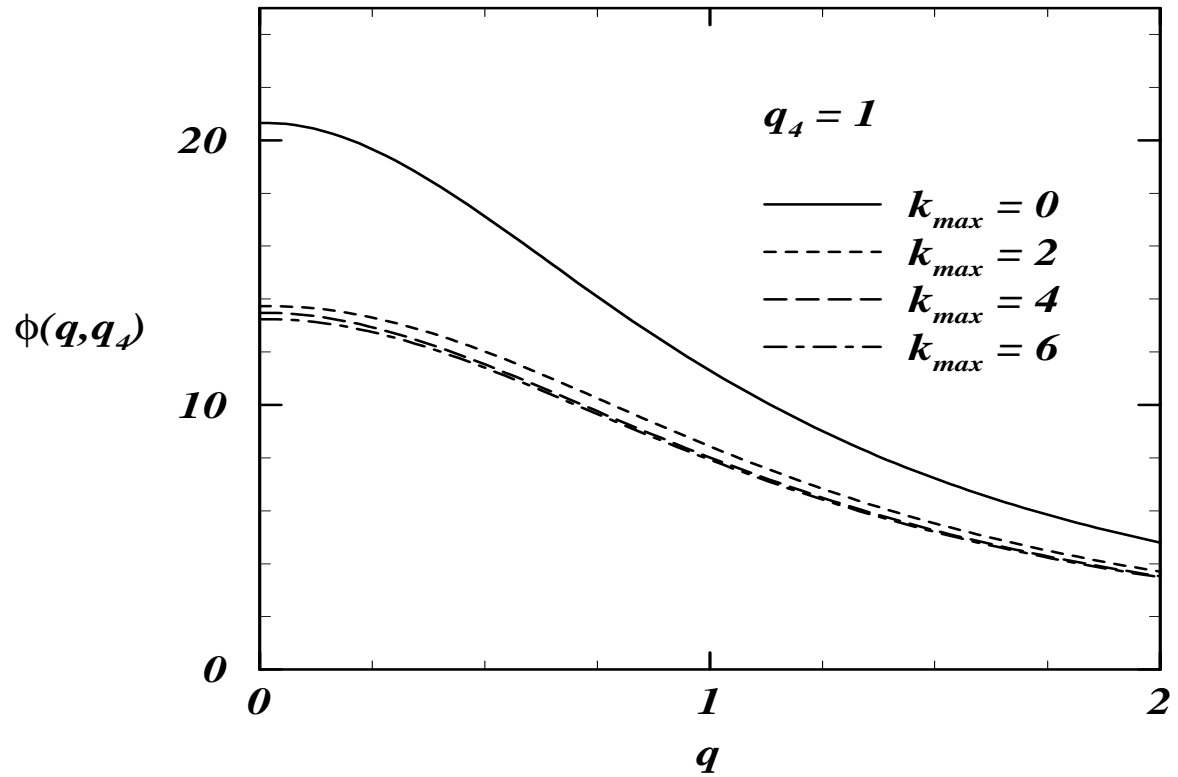
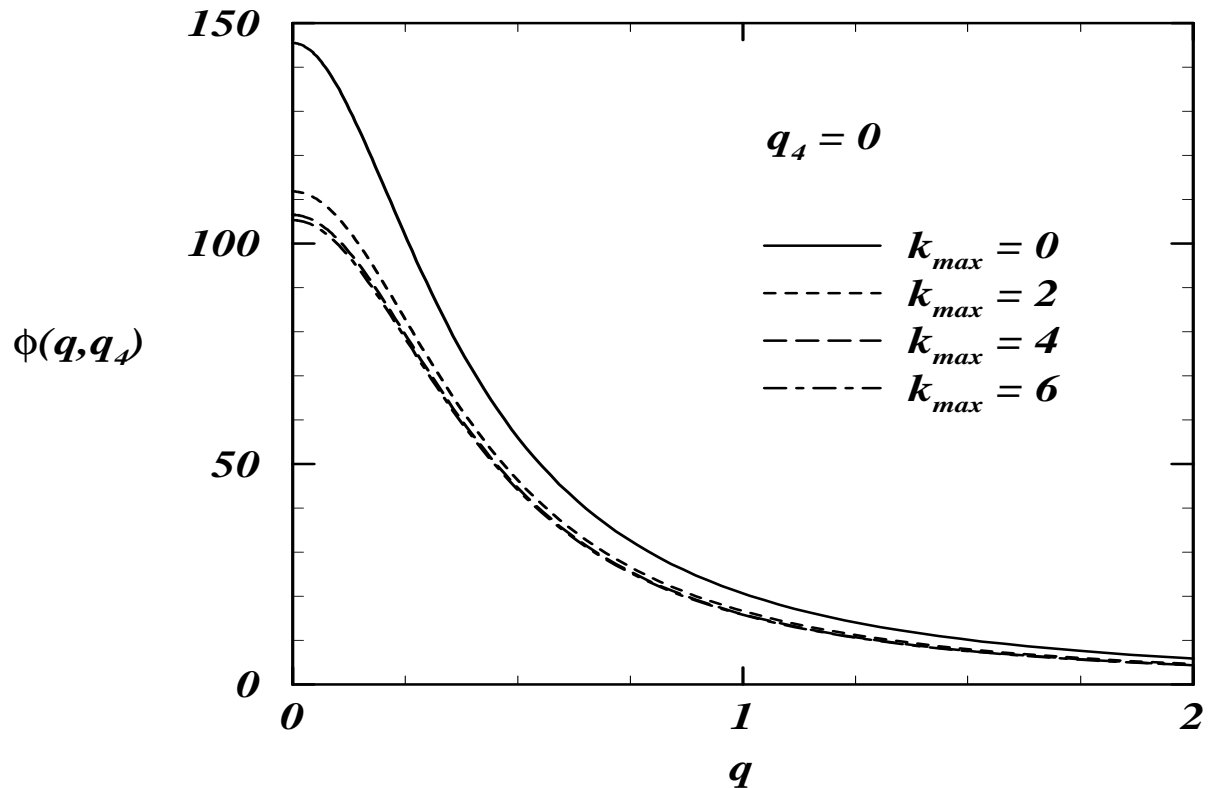


FIG. 2. Rate of convergence of hyperspherical expansion of the vertex functions $\Phi(\mathbf{q}, q_4)$ for $\mu/m = 0.1$, $M/m = 1.9$ and $l = 0$ at $q_4 = 0$ and 1. Note the different scales on the vertical axis.

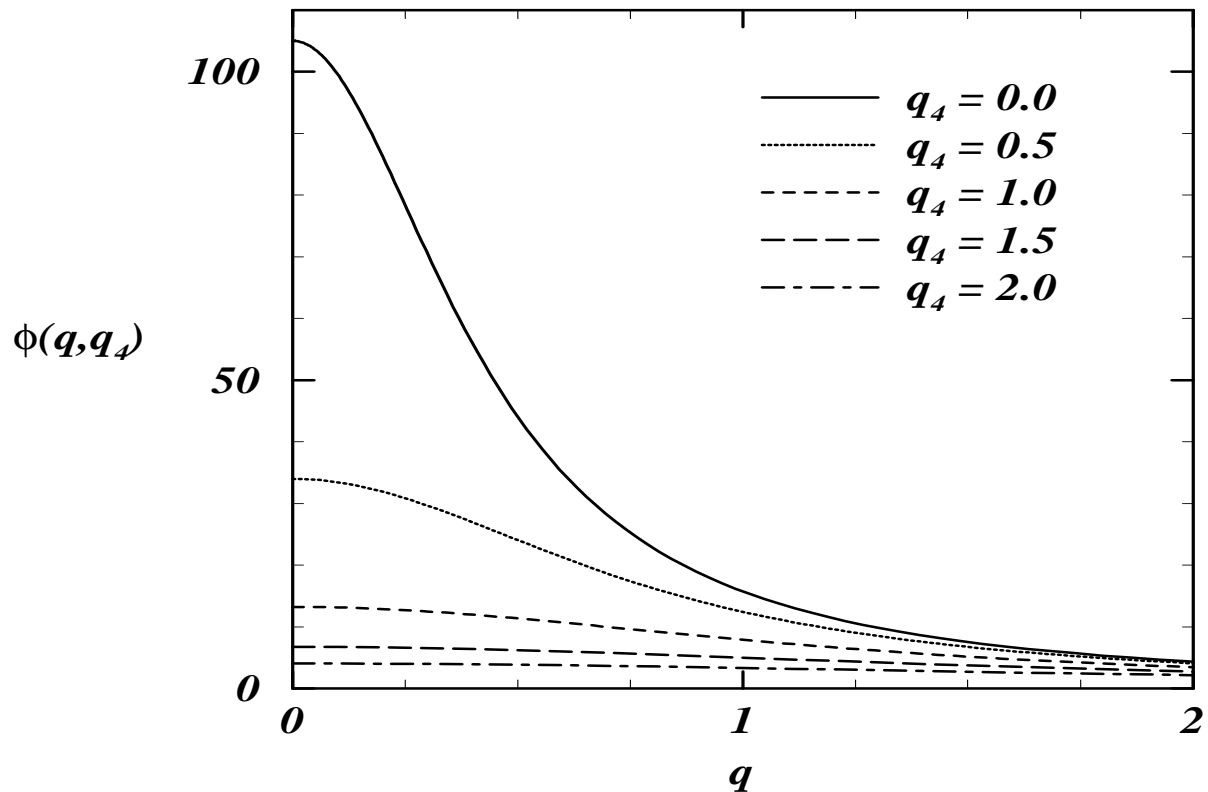


FIG. 3. The $|\mathbf{q}|$ and q_4 dependence of the vertex function $\Phi(q, q_4)$ for $\mu/m = 0.1$, $M/m = 1.9$ and $l = 0$ at various values of the relative energy q_4 .

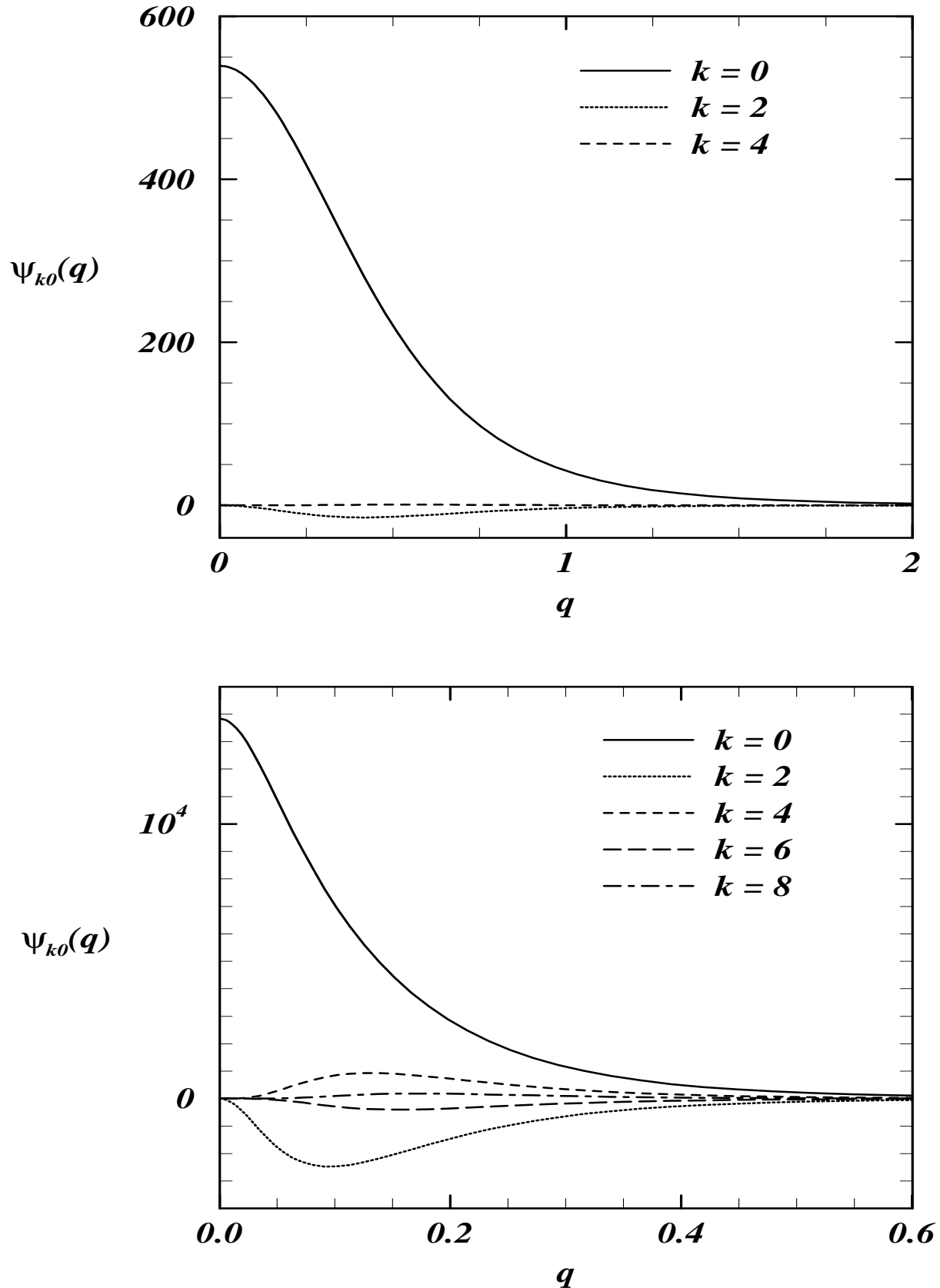


FIG. 4. Hyperspherical components of the wave function $\Psi_{k0}(q)$ for $\mu/m = 0.1$ and $l = 0$. The upper graph is for the case $M/m = 1$ while the lower one contains the solutions for $M/m = 1.9$.

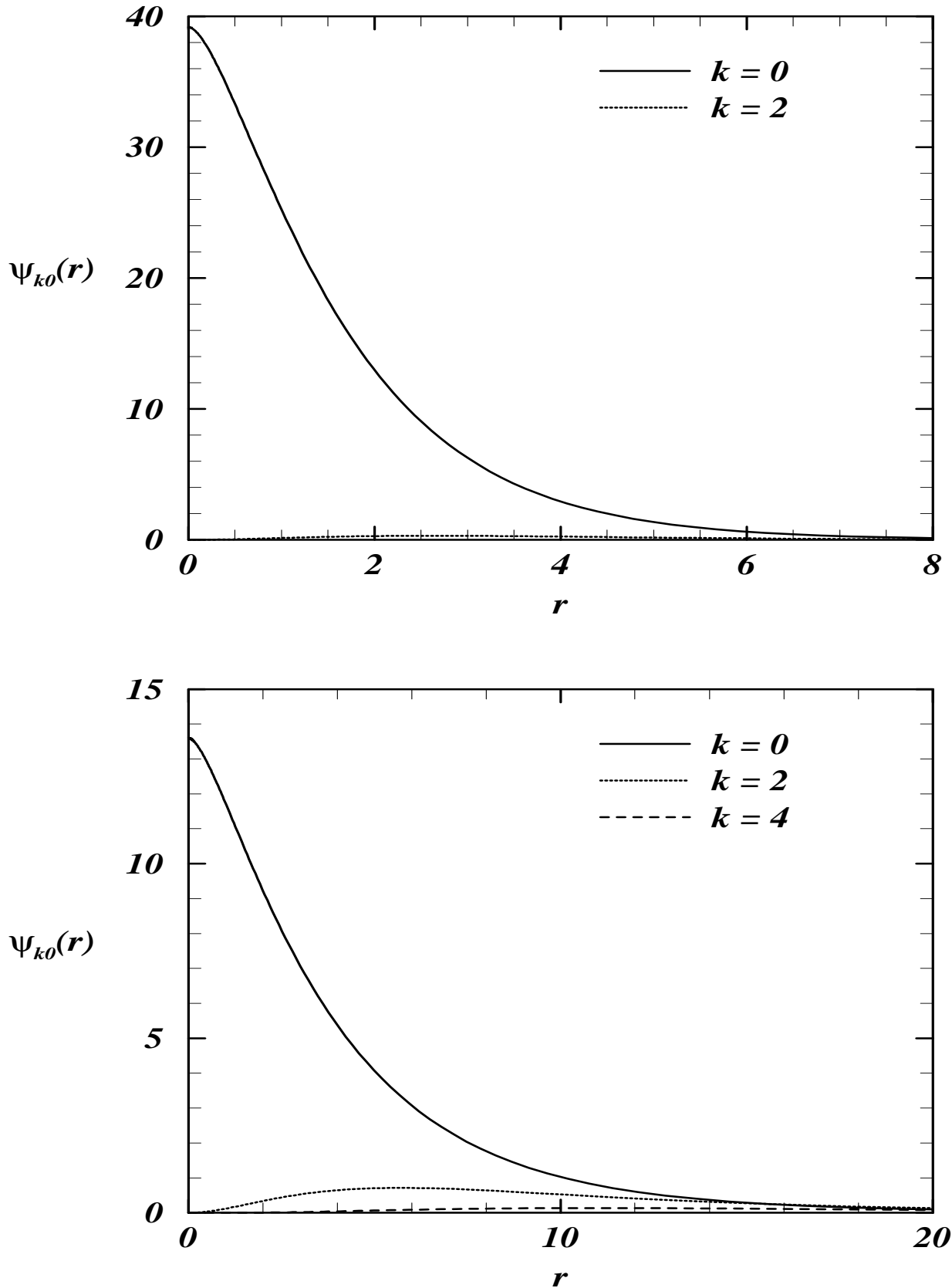


FIG. 5. Hyperspherical components of the configuration space wave function for $\mu/m = 0.1$ and $l = 0$. The upper graph shows the components $\hat{\Psi}_{k0}(r)$ for $M/m = 1$ while the lower one contains the solutions for $M/m = 1.9$.

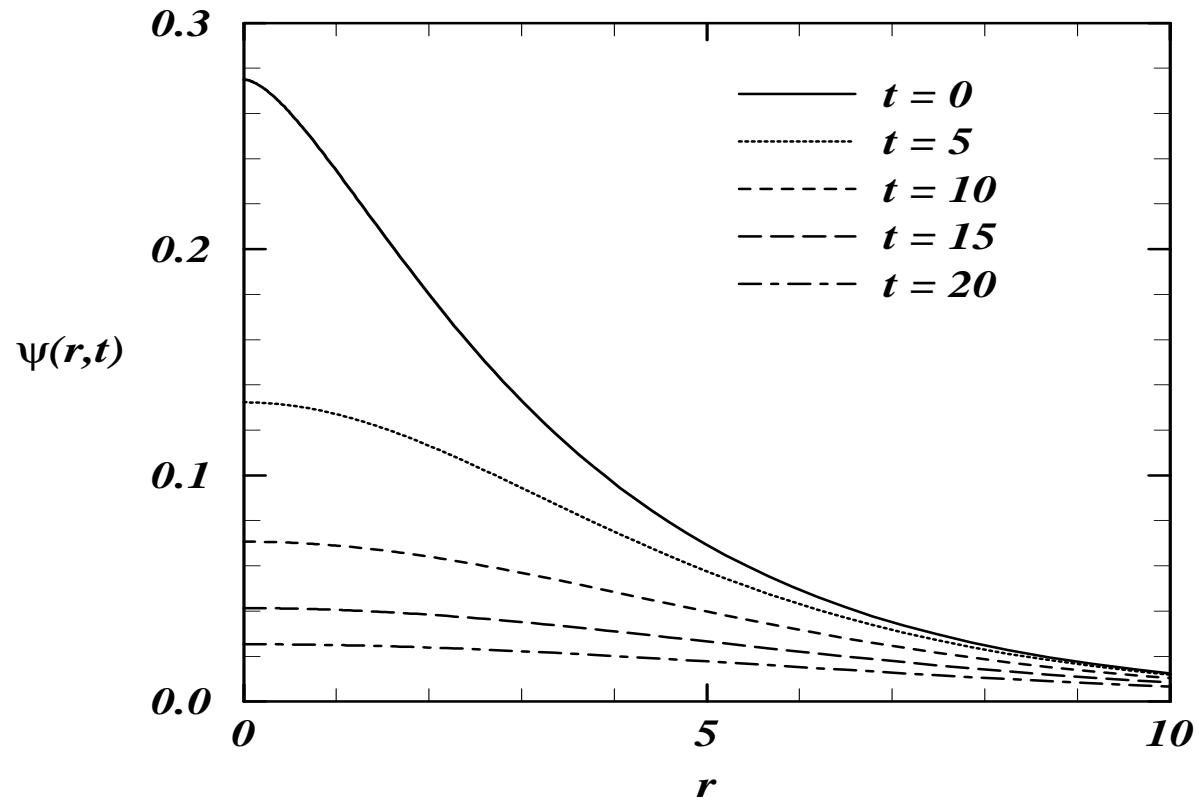


FIG. 6. The $|\mathbf{r}|$ and t dependence of the configuration space wave function $\Psi_0(|\mathbf{r}|, t)$ for $\mu/m = 0.1$, $M/m = 1.9$ and $l = 0$ at various values of the relative time t .

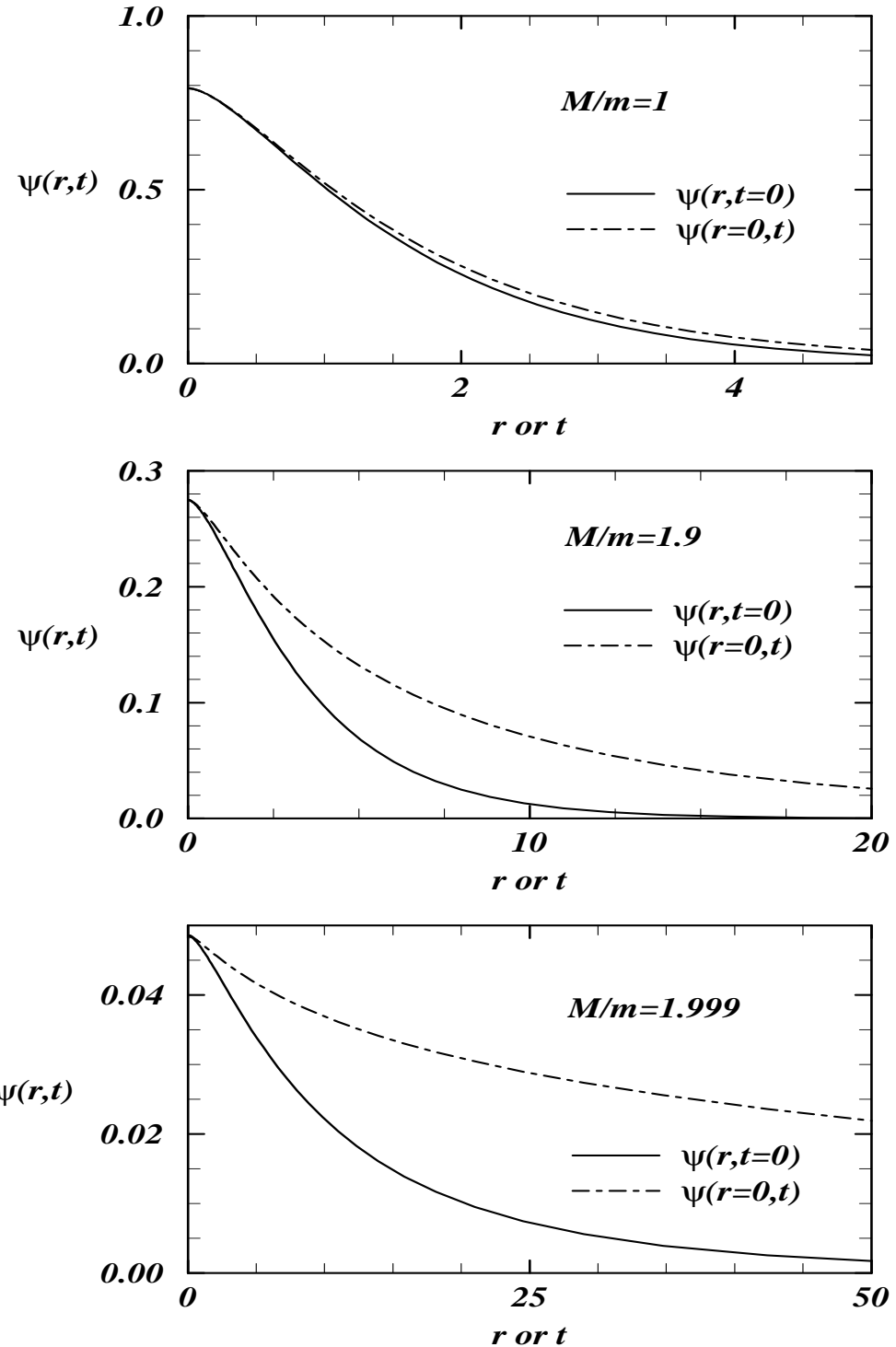


FIG. 7. Comparison of the relative time zero wave function $\Psi_0(|\mathbf{r}|, t = 0)$ with the relative distance zero wave function $\Psi_0(r = 0, t)$ for $\mu/m = 0.1$ and $l = 0$. In the nonrelativistic limit $M/m \rightarrow 2$, $\Psi_0(|\mathbf{r}|, t)$ is seen to become less dependent on t .